

Measurements of angular distributions for ${}^7\text{Li}$ elastically scattered from ${}^{58}\text{Ni}$ at energies around the Coulomb barrier

P Amador-Valenzuela¹, E F Aguilera¹, E Martinez-Quiroz¹, D Lizcano¹ and J C Morales-Rivera^{1,2}

¹ Departamento de Aceleradores, Instituto Nacional de Investigaciones Nucleares, Apartado Postal 18-1027, C.P. 11801, Ciudad de México, México

² Facultad de Ciencias, Universidad Autónoma del Estado de México, C.P. 50000, Toluca, Estado de México

E-mail: paulina.amador@inin.gob.mx, eli.aguilera@inin.gob.mx

Abstract. Recently, experimental measurements of elastic scattering angular distributions for the system ${}^7\text{Li}+{}^{58}\text{Ni}$ at ten different energies around the Coulomb barrier were made by the Heavy-Ion Group. The measurements were made at the Tandem Van de Graaff Particle Accelerator Laboratory in the National Institute for Nuclear Research (ININ) in Mexico. In this work, preliminary elastic scattering angular distributions for five energies ($E_{lab} = 12.0, 12.5, 13.0, 13.5$ and 14.22 MeV) are presented. The preliminary experimental data were analyzed using the São Paulo Optical Model Potential (SPP) which is based on a double-folding potential, reproducing very well these data. A comparison is made with old data reported back in 1973 and in 2012. Further analysis is in progress in order to fully understand this particular system, specially because ${}^7\text{Li}$ is known to be a weakly bound nucleus.

1. Introduction

In nuclear physics, elastic scattering experiments are of great importance since valuable information on the properties of the nucleus can be obtained through them. A clear and specific example of the relevance of elastic scattering experiments is the discovery of the atomic nucleus in 1911, made by Ernest Rutherford. Lately, many experiments and theoretical analyse have been performed using radioactive beams as projectiles to produce a nuclear reaction [1, 2, 3, 4, 5, 6, 7, 8, 9, 10, 11, 12, 13, 14, 15, 16]. It is well known that in general experiments with halo nuclei are difficult to carry out, mainly because of the low intensities of the respective beams. It is also known that halo nuclei (cluster-type nuclei) have a relative small separation energy which means that the probability of breakup is important in the presence of the force field produced by the target. With this in mind, information on the effect of coupling to the breakup channel becomes essential when dealing with radioactive beams of this kind. This effect can first be investigated using stable weakly bound beams which have much higher intensities than radioactive beams. The suitable stable nuclei for this kind of study are ${}^9\text{Be}$, ${}^6\text{Li}$ and ${}^7\text{Li}$ with separation energies of 1.57, 1.47 and 2.47 MeV, respectively.

Recently, many experiments of elastic scattering between heavy ions, using strongly bound nuclei, at energies near the Coulomb barrier have been performed. The analysis of these



experiments present a systematic behaviour of the energy dependence of the interacting optical potential known as the Threshold Anomaly (TA) [17]. Basically, the threshold anomaly implies a rapid variation of the optical potential (real and imaginary part) extracted from the analysis of the experimental data when the energy decreases towards the Coulomb barrier. For the real part of the potential there is a localized peak (bump) at the barrier energy, whereas there is a sharp decrease of the imaginary part of this potential. The decrease of the imaginary potential can be understood as the closure of the non-elastic channels at energies below the Coulomb barrier [18, 19]. For weakly bound nuclei the breakup channel is expected to be a relevant reaction channel even at energies below the Coulomb barrier. Since the coupling to the breakup channel produces a repulsive polarization potential then there is a big probability that the threshold anomaly may disappear. It has been suggested that a new type of anomaly is present in the scattering of weakly bound nuclei, named as breakup threshold anomaly [20]. In this anomaly the strength of the imaginary potential increases as the incident energy decreases, at energies below the Coulomb barrier.

For ${}^6\text{Li}$ projectiles, it has been shown that the threshold anomaly does not appear irrespective of whether it is incident on a heavy or light target [19, 20, 21, 22, 23, 24, 25, 26, 27, 28]. As for ${}^7\text{Li}$ the conclusions seem to be different since it has been shown that the behaviour does depend on the mass of the target. This point has been discussed with detail elsewhere [19, 21]. As already mentioned, elastic scattering measurements of weakly bound nuclei at energies around the Coulomb barrier are of great importance. For doing theoretical analyse, such as an analysis of the threshold anomaly or breakup threshold anomaly, a good set of data points, that is, complete elastic scattering angular distributions at several energies are always helpful. In this context, it came to our attention that the information existent on elastic scattering angular distributions covering a wide angular range for ${}^7\text{Li}$ on medium targets at energies below the Coulomb barrier is very scarce. Most of the measurements reported correspond to energies near but above the Coulomb barrier; ${}^7\text{Li}+{}^{58}\text{Ni}$ [29], ${}^7\text{Li}+{}^{59}\text{Co}$ [26], ${}^7\text{Li}+{}^{64}\text{Ni}$ [21]. In addition, the measurements reported for energies near but below the Coulomb barrier for ${}^7\text{Li}+{}^{58}\text{Ni}$ are not full angular distributions as reported by Zerva K *et al.* [30], where the elastic backscattering technique is used. With this in mind, recently the Heavy-Ion Group made full experimental elastic scattering measurements for the system ${}^7\text{Li}+{}^{58}\text{Ni}$ at ten different energies around and below the Coulomb barrier ($V_b = 14.0$ MeV in the laboratory frame of reference). The measurements were made at the Tandem Particle Accelerator Laboratory in the National Institute for Nuclear Research (ININ) in Mexico. In this work, we present preliminary angular distributions of ${}^7\text{Li}$ elastically scattered from ${}^{58}\text{Ni}$ for five out of the ten energies measured. Preliminary calculations using the optical model potential (OMP) are also reported as well as a comparison with data reported by Pfeiffer K O *et al.* [29] and by Zerva K *et al.* [30].

2. Experimental setup

The experiment took place at the particle accelerator laboratory in the National Institute for Nuclear Research in Mexico. This particular accelerator, used during the experiment, is a Tandem Van de Graaff with a nominal maximum operational voltage of 6 MV and is the only one in Mexico that produces stable beams of heavy ions (from hydrogen to carbon) at energies around the barrier, of great interest depending on the system. The ${}^7\text{Li}$ beam current, produced by the particle accelerator, had intensities from 10 to 20 pA depending on the energy. Two different targets were used, one of them was a gold foil (${}^{197}\text{Au}$) with an approximate thickness of 1.11 mg/cm^2 and the other one was an enriched (99.9%) ${}^{58}\text{Ni}$ foil with a nominal thickness of 0.259 mg/cm^2 . The gold target was used for solid angle determination. The measurements were made in a 70 cm diameter scattering chamber (experimental line of 30°), at ten different energies being 9.0 and 14.22 MeV (laboratory frame of reference) the lowest and highest energy, respectively, with steps of 0.5 MeV between 10 and 13.5 MeV. Inside the chamber (2π geometry),

a circular table and a target holder are located, and both of them can be rotated to any desired angle. The detectors can be placed on the circular table at different angular positions. The size of the beam was defined by a set of vertical and horizontal slits placed on the wall of the chamber with an aperture of $3 \text{ mm} \times 3 \text{ mm}$.

The scattered particles were detected with six silicon surface-barrier (SSB) detectors. Four of them were placed at forward angles and two at backward angles with respect to the beam axis as shown in figure 1. In a first experimental setup (configuration) the position of the normal to the target was set at 10° with respect to the ${}^7\text{Li}$ beam axis, and the positions of each of the six detectors were 35° (det. A), 45° (det. B), 55° (det. C), 65° (det. D), 155° (det. E) and 165° (det. F), respectively. After the measurements were made with this first configuration, the circular table and target holder were rotated to a second configuration, leaving the target at 40° and the detectors at 65° (det. A), 75° (det. B), 85° (det. C), 95° (det. D), 120° (det. E) and 135° (det. F) with respect to the beam axis, respectively. This procedure was repeated for all the energies measured. The solid angles subtended by the detectors at the target center were 2.25, 5.69, 2.03, 1.90, 7.26 and 3.3 msr for detectors A, B, C, D, E and F, respectively.

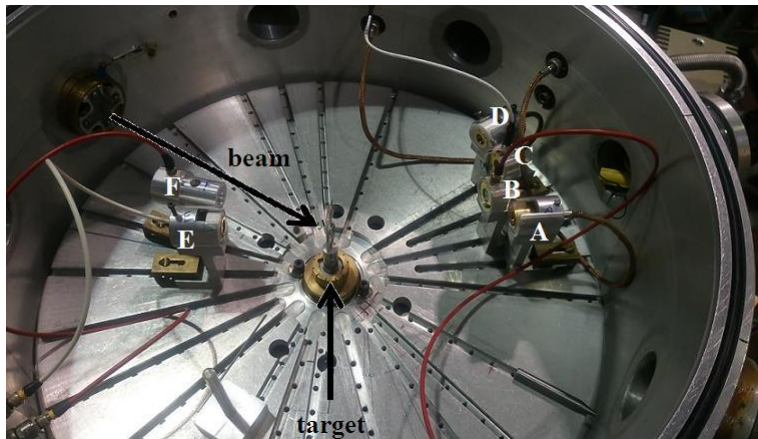


Figure 1. Scattering chamber showing the experimental setup.

3. Results and discussion

The preliminary elastic scattering angular distributions measured at the energies of 12.0, 12.5, 13.0, 13.5 and 14.22 MeV in the laboratory frame of reference are shown in figure 2. The total error reported considers the statistical and systematic errors which in some cases are smaller than the symbols as shown in the figure. These preliminary angular distributions were normalized to Rutherford scattering at the lowest angle measured to allow the determination of deviations from pure Coulomb scattering.

The experimental data were analyzed using the double-folding São Paulo Potential (SPP) [31, 32] for the real part of the nuclear interaction, and a standard Woods-Saxon (WS) shape for the imaginary part. The values of the potential parameters obtained for the imaginary part are indicated in table 1, where W is the depth, R_i is the radius and a_i the diffuseness of the potential. The respective calculations are represented by the curves shown in figure 2. For all five energies it was possible to fit the data using the same value for the parameters of the imaginary part of the potential, as shown in table 1. It can be seen from figure 2 that the calculations obtained in this work describe very well the preliminary experimental data for the ${}^7\text{Li}+{}^{58}\text{Ni}$ system. All χ^2/N values reported here refer to χ^2 per point. The total reaction cross sections (σ_R) for each energy are also given in table 1.

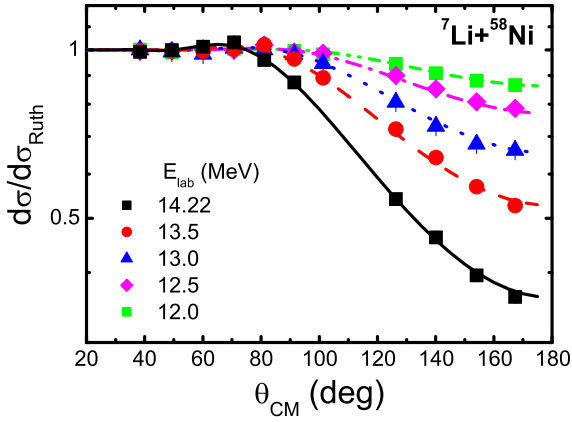


Figure 2. Preliminary elastic scattering angular distributions for ${}^7\text{Li}+{}^{58}\text{Ni}$ at the five energies indicated. The curves correspond to optical model calculations using the São Paulo Potential (SPP) for the real part and a Woods-Saxon shape for the imaginary part (the parameters are shown in table 1).

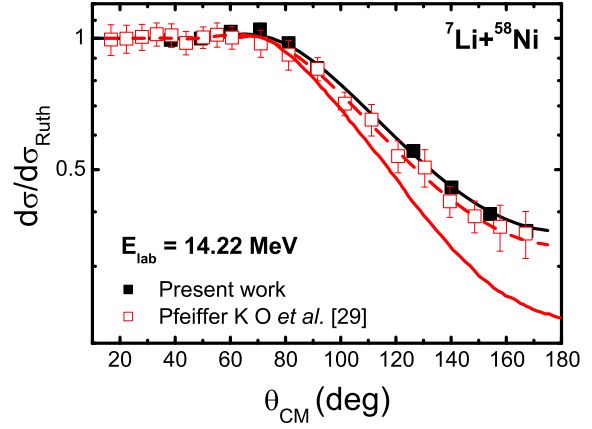


Figure 3. Comparison of the elastic scattering angular distribution for $E_{lab} = 14.22$ MeV between data reported in the present work and those by Pfeiffer K O *et al.* [29]. The curves (black solid line and red dashed line) correspond to optical model calculations using the SPP for the real part and a Woods-Saxon shape for the imaginary part for each set of experimental points (the parameters are shown in table 1). The red solid line corresponds to optical model calculations reported in Ref. [29], see text for further information.

Table 1. Optical-model potential obtained for ${}^7\text{Li}+{}^{58}\text{Ni}$ from the present data and the calculated total reaction cross sections for each energy. The SPP is used for the real part and a Woods-Saxon shape for the imaginary part.

E_{lab} (MeV)	W (MeV)	R_i (fm)	a_i (fm)	χ^2/N	σ_R (mb)
12.0	60	1.2	0.56	0.18	32 ± 13
12.5	60	1.2	0.56	0.46	58 ± 12
13.0	60	1.2	0.56	0.75	96 ± 12
13.5	60	1.2	0.56	1.06	148 ± 12
14.22	60	1.2	0.56	0.56	239 ± 13
14.22*	60	1.2	0.60	0.08	281 ± 84

* experimental data reported by Pfeiffer K O *et al.* [29]

As part of the analysis presented in this work, a comparison of the elastic scattering angular distribution for $E_{lab} = 14.22$ MeV between data reported by Pfeiffer K O *et al.* [29] and the present work was made, as shown in figure 3. From this figure, it is possible to see that the preliminary experimental data reported in this work, for this energy, are in good agreement

with respect to the data reported back in 1973 by Pfeiffer K O *et al.* [29]. The latter data were also analyzed using the SPP for the real part and a WS shape for the imaginary part of the potential (red dashed line), the respective parameters are also shown in table 1. It can be seen from the table that the only parameter that had to be modified in order to get the best fit for these experimental data was the diffuseness (from 0.56 to 0.6 fm). The total reaction cross section obtained with the SPP for the real part and the WS for the imaginary part of the potential gives a value of 281 mb while Pfeiffer K O *et al.* [29] reports a value of 420 mb. In figure 3, it is possible to observe that the elastic scattering angular distribution fit (red solid line) reported in Ref. [29] fails to reproduce the experimental data at angles above 80° (center of mass reference frame), which explains the large difference in the above reaction cross section values. The red solid curve of figure 3 was directly extracted from figure 4b of Ref. [29]. In Pfeiffer's work, a normal volume Woods-Saxon shape for the real and imaginary parts of the optical potential was used to analyze the experimental elastic scattering angular distributions (see table 3 of Ref. [29]). The WS parameters reported by Pfeiffer for the energy of 14.22 MeV were $V = 152$ MeV, $r_r = 1.32$ fm and $a_r = 0.79$ fm for the real part, and $W = 3.65$ MeV, $r_i = 2.48$ fm and $a_i = 0.49$ fm for the imaginary part. Throughout Pfeiffer's analysis the value of the radius was calculated as $R = r_0 A_t^{1/3}$, where A_t is the target mass and the value of the reduced radius used was $r_0 = 1.25$ fm. Using these parameter values, we were able to reproduce the red solid line of figure 3.

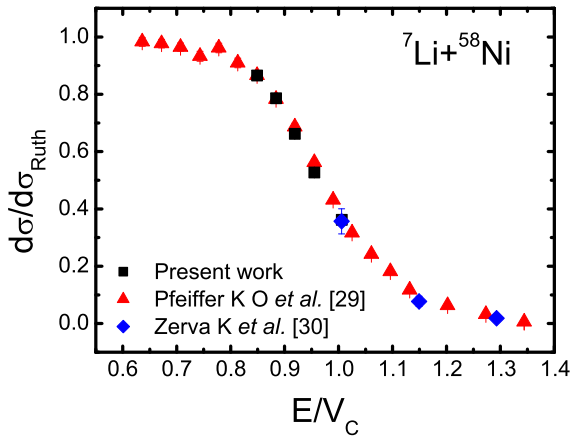


Figure 4. Comparison of the excitation functions of average cross sections between 160° and 170° for the ${}^7\text{Li}+{}^{58}\text{Ni}$ system. The experimental data points reported in the present work and those reported by Ref. [29] are measurements taken from full angular distributions.

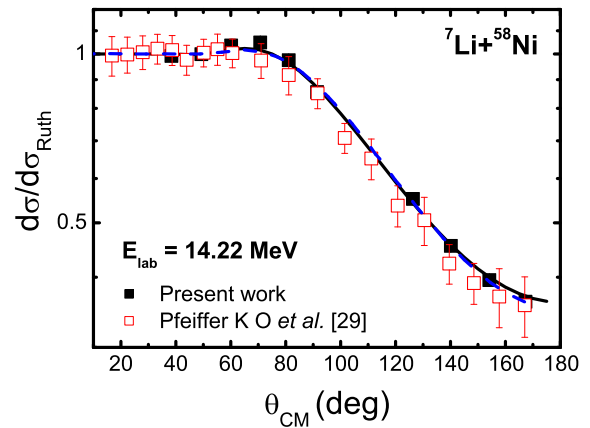


Figure 5. Elastic scattering angular distribution for $E_{lab} = 14.22$ MeV reported in this work and by Pfeiffer K O *et al.* [29]. Calculations using the São Paulo Potential (SPP) for the real part and a Woods-Saxon shape for the imaginary part of the nuclear potential (black solid line) and data extracted from Ref. [30] (blue dashed line), see text for further information.

On the other hand, Zerva K *et al.* [30] performed precision elastic backscattering measurements for the ${}^7\text{Li}+{}^{58}\text{Ni}$ system at energies from 9.0 MeV to 19.0 MeV in the laboratory frame of reference. In that work, the excitation function of average cross-sections between 160° and 170° for the ${}^7\text{Li}+{}^{58}\text{Ni}$ system was reported. Since in Pfeiffer K O *et al.* [29] as well as in the present work, the full elastic scattering angular distributions for ${}^7\text{Li}+{}^{58}\text{Ni}$ are reported, it was

possible to extract the excitation function and compare with Zerva's experimental data. This comparison is shown in figure 4. For this comparison, a value of $V_C = 14.14$ MeV (laboratory frame of reference) for the Coulomb barrier of the ${}^7\text{Li}+{}^{58}\text{Ni}$ system was used, as indicated in Ref. [30]. When comparing the excitation function from the present work with those from Pfeiffer K O *et al.* [29] and Zerva K *et al.* [30] it is possible to see that the data points are in good agreement in the small angular range considered ($160^\circ - 170^\circ$).

In addition, Zerva K *et al.* compared the elastic scattering angular distributions reported in 1973 by Pfeiffer K O *et al.* with optical model predictions using the potentials obtained via the backscattering barrier distribution technique (see Ref. [30] for details). The mentioned predictions (blue dashed line) for $E_{lab} = 14.22$ MeV reported by Zerva as well as the experimental data reported by Pfeiffer and the preliminary experimental data reported in this work are shown in figure 5. The prediction found by Zerva fails to reproduce Pfeiffer's experimental data as shown in figure 5. This in fact is indicated in Zerva's work, since it is stated that despite several trial attempts it was impossible to find a potential which described the experimental data reported by Pfeiffer *et al.* and that this was a possible indication that new angular distribution measurements may be necessary. Following Zerva's statement and as part of the motivation for this experiment, it can be seen from the same figure that the preliminary experimental data for $E_{lab} = 14.22$ MeV reported in this work are well reproduced by the prediction reported in Zerva's work. At the same time, the optical model predictions obtained in the present work are also in agreement with Zerva's prediction. This can be seen as an indication that the new experimental data, for the system ${}^7\text{Li}+{}^{58}\text{Ni}$, is a reliable set of data points which may be used for analysis of the threshold anomaly or breakup threshold anomaly.

4. Conclusions

Recently, measurements of ${}^7\text{Li}$ elastically scattered from ${}^{58}\text{Ni}$ at energies near and below the Coulomb barrier were made. In the present work, preliminary elastic scattering angular distributions for five out of ten energies were reported. By using the double-folding São Paulo potential for the real part of the nuclear interaction and a Woods-Saxon shape for the imaginary part, the five preliminary angular distributions were well described. The comparison between full and partial ($160^\circ - 170^\circ$) experimental angular distributions for $E_{lab} = 14.22$ MeV reported back in 1973 [29] and in 2012 [30], respectively, are in good agreement with the full preliminary data reported in the present work. Further analysis is in progress in order to further understand this particular system.

Acknowledgments

The authors would like to acknowledge the staff of the Tandem Van de Graaff particle accelerator at ININ for all their support and time dedication during this experiment. This work was partially supported by CONACYT.

References

- [1] Canto L F, Gomes P R S, Donangelo R and Hussein M S 2006 *Phys. Rep.* **424** 1
- [2] Keeley N, Raabe R, Alamanos N and Sida J L 2007 *Part. Nucl. Phys.* **59** 579
- [3] Keeley N, Alamanos N, Kemper K and Rusek K 2009 *Part. Nucl. Phys.* **63** 396
- [4] Aguilera E F *et al.* 2000 *Phys. Rev. Lett.* **84** 5058
- [5] Aguilera E F *et al.* 2001 *Phys. Rev. C* **63** 061603(R)
- [6] Kolata J J *et al.* 1998 *Phys. Rev. Lett.* **81** 4580
- [7] De Young P A *et al.* 2005 *Phys. Rev. C* **71** 051601(R)
- [8] Guimarães V *et al.* 2000 *Phys. Rev. Lett.* **84** 1862
- [9] Aguilera E F *et al.* 2009 *Phys. Rev. C* **79** 021601(R)
- [10] Aguilera E F *et al.* 2011 *Phys. Rev. Lett.* **107** 092701
- [11] Pakou A *et al.* 2013 *Phys. Rev. C* **87** 014619

- [12] Fernández-García J P , Rodríguez-Gallardo M, Alvarez M A G and Moro A M 2010 *Nucl. Phys. A* **840** 19–38
- [13] Sánchez-Benítez A M *et al.* 2008 *Nucl. Phys. A* **803** 30–45
- [14] Milin M *et al.* 2004 *Nucl. Phys. A* **730** 285–298
- [15] Kakuee O R *et al.* 2003 *Nucl. Phys. A* **728** 339–349
- [16] Benjamim E A *et al.* 2007 *Phys. Lett. B* **647** 30–35
- [17] Satchler G R 1991 *Phys. Rep.* **199** 147
- [18] Gomes P R S and Lubian J 2014 *J. Phys.: Conf. Series* **533** 012029
- [19] Di Pietro A 2010 *J. Phys.: Conf. Series* **205** 012042
- [20] Hussein M S *et al.* 2006 *Phys. Rev. C* **73** 044610
- [21] Shaikh Md. Moin, Das Mili, Roy Subinit, Sinha M, Pradhan M K, Basu P, Datta U, Ramachandran K, Shrivastava A 2016 *Nucl. Phys. A* **953** 80–94
- [22] Keeley N, Bennett S J, Clarke N M, Fulton B R, Tungate G, Drumm P V, Nagarajan M A and Lilley J S, 1994 *Nucl. Phys. A* **571** 326
- [23] Maciel A M M *et al.* 1999 *Phys. Rev. C* **59** 2103
- [24] Pakou A *et al.* 2004 *Phys. Rev. C* **69** 054602
- [25] Figueira J M *et al.* 2007 *Phys. Rev. C* **75** 017602
- [26] Souza F A, Leal L A S, Carlin N, Munhoz M G, Liguori Neto R, de Moura M M, Suaide A A P, Szanto E M, Szanto de Toledo A and Takahashi J 2007 *Phys. Rev. C* **75** 044601; 2007 *Phys. Rev. C* **76** 029901(E)
- [27] Biswas M, Roy Subinit, Sinha M, Pradhan M K, Mukherjee A, Basu P, Majumdar H, Ramachandran K and Shrivastava A 2008 *Nucl. Phys. A* **802** 67–81
- [28] Deshmukh N N *et al.* 2011 *Phys. Rev. C* **83** 024607
- [29] Pfeiffer K O, Speth E and Bethge K 1973 *Nucl. Phys. A* **206** 545–557
- [30] Zerva K *et al.* 2012 *Eur. Phys. J. A* **48** 102
- [31] Chamon L C, Pereira D, Hussein M S, Cândido Ribeiro M A and Galetti D (1997) *Phys. Rev. Lett.* **79** 5218
- [32] Chamon L C, Carlson B V, Gasques L R, Pereira D, De Conti C, Alvarez M A G, Hussein M S, Cândido Ribeiro M A, Rossi Jr. E S and Silva C P 2002 *Phys. Rev. C* **66** 014610
- [33] Thompson I J 1988 *Comput. Phys. Rep.* **7** 167–212